Inorganic Chemistry

ARTICLE

pubs.acs.org/IC

S_T = 22 [Mn_{10}] Supertetrahedral Building-Block to Design Extended Magnetic Networks

Gang Wu,*[,†] Jian Huang,[†] Linlin Sun,[†] Jiaquan Bai,[†] Guanghua Li,[†] Eduard Cremades,[‡] Eliseo Ruiz,[‡] Rodolphe Clérac,*[,§,⊥] and Shilun Qiu[†,*]

[†]State Key Laboratory of Inorganic Synthesis & Preparative Chemistry, Jilin University, 2699 Qianjin Street, 130012 Changchun, China

[‡]Departament de Química Inorgànica and Institut de Recerca de Química Teòrica i Computacional, Universitat de Barcelona, Diagonal 647, 08028 Barcelona, Spain

[§]Centre de Recherche Paul Pascal, CNRS, UPR-8641, 115 avenue du Dr. Albert Schweitzer, 33600 Pessac, France

[⊥]Université de Bordeaux, UPR-8641, 33600 Pessac, France

Supporting Information

ABSTRACT: The controlled organization of high-spin complexes, eventually single-molecule magnets, is a great challenge in molecular sciences to probe the possibility to design sophisticated magnetic systems to address a large quantity of magnetic information. The coordination chemistry is a tool of choice to make such materials. In this work, high-spin S_T = 22 [Mn_{10}] complexes, such as $[Mn^{III}_6Mn^{II}_4(L_1)_6(\mu_4\text{-}O)_4(\mu_3\text{-}N_3)_4(CH_3CN)_{11}(H_2O)]\cdot(ClO_4)_2\cdot(CH_3CN)_{8.5}$ (**1**), have been assembled using (i) 1,3-propanediol derivatives as chelating ligands to form the [Mn_{10}] core units and (ii) dicyanamide or azide anions as linkers to synthesize the first 2D and 3D [Mn_{10}]-based networks: $[Mn^{III}_6Mn^{II}_4(L_2)_6(\mu_3\text{-}N_3)_4(\mu_4\text{-}O)_4(CH_3OH)_4(dca)_2]$ (**2**) and $[Mn^{III}_6Mn^{II}_4(L_3)_6(\mu_3\text{-}N_3)_4(\mu_4\text{-}O)_4(N_3)_2]\cdot(CH_3OH)_4$ (**3**). The synthesis of these compounds is reported together with their single-crystal X-ray structures and magnetic properties supported by DFT calculations. In the reported synthetic conditions, the stability of the [Mn_{10}] complex is remarkably good that allows us to imagine many new materials combining these high-spin moieties and other diamagnetic but also paramagnetic linkers to design for example ordered magnets.

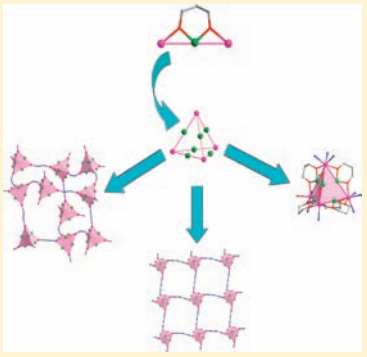

INTRODUCTION

Single-molecule magnets (SMMs) are molecules with a high-spin ground state and uniaxial anisotropy, which lead to slow relaxation of their magnetization.[1] Therefore, they can act as monodisperse superparamagnetic particles for high-density magnetic data storage at the molecular level.[1b,c] After the pioneering works of W. Wernsdorfer and G. Christou,[2] who have studied supramolecular dimers and 3D arrangements of SMMs, the organization of SMMs or high-spin complexes into supramolecular or coordination networks becomes a new objective for chemists to combine the intrinsic magnetic properties of such unique building-blocks and intercomplex magnetic interactions to stabilize new magnetic behaviors.[3] Despite these exciting developments, extended networks based on known SMMs or high-spin complexes are extremely rare due to the difficulties to control the organization of such species even using directional linkers between magnetic objects.[3]

Recently, a series of large polynuclear complexes based on a supertetrahedron $[Mn^{III}_6Mn^{II}_4]$ motif (Figure 1, Mn^{II} and Mn^{III} occupying the vertices and edges of the supertetrahedron, respectively) has been reported to display remarkable magnetic properties.[4] The interactions present in this $[Mn^{III}_6Mn^{II}_4]$ core are ferromagnetic inducing a large spin ground state such as S_T = 22 for individual [Mn_{10}] complexes.[4a,b] The condensation of two [Mn_{10}] units by a sharing Mn^{II} vertices leads to a [Mn_{19}] complex that displays so far the highest spin ground state known for a molecular object: S_T = 83/2.[4c] [Mn_{17}] aggregates composed of two edge sharing [Mn_{10}] supertetrahedra have also been reported.[3m,4d] Combined magnetic measurements and DFT calculations confirmed dominating intracomplex ferromagnetic interactions and its S_T = 37 spin ground state.[4d,e] Corner- or edge-sharing assemblage of molecular units into larger polyhedral arrangements with certain control over the topology of the final polynuclear cores is very common in chalcogenidometallate and polyoxometallates (POMs) chemistry[5] but still very rare for open-shell transition-metal complexes.[6] Therefore, the synthesis of [Mn_{10}] supertetrahedron-based compounds is clearly a challenge in manganese coordination chemistry toward the synthesis of new $[Mn_{10}]_n$ magnetic complexes and networks. Herein, we present a series of materials based on the supertetrahedron [Mn_{10}] motif using (i) 1,3-propanediol derivatives (Chart 1) as chelating ligands to form the [Mn_{10}] core unit and (ii) dicyanamide or azide anions as linkers to synthesize the first 2D and 3D [Mn_{10}]-based networks (Figure 1).

Received: May 30, 2011
Published: August 05, 2011

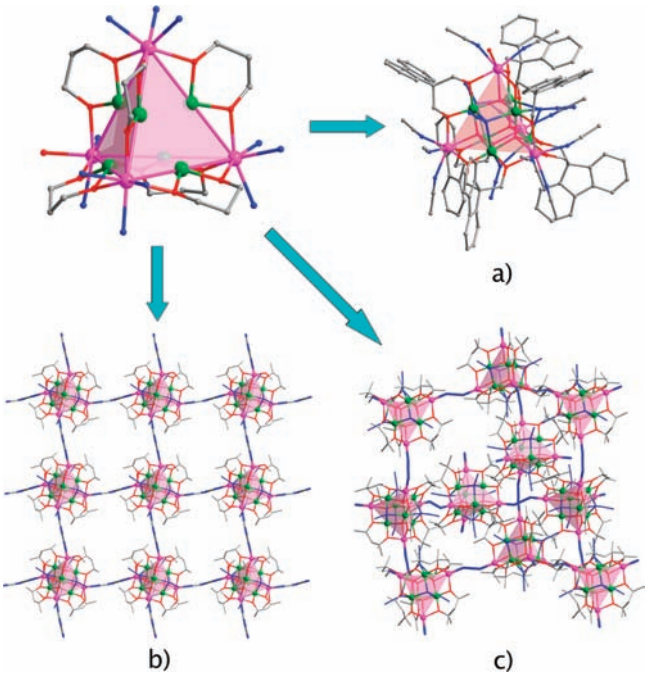

Figure 1. Structures of the materials based on the S_T = 22 [Mn_{10}] repeating units with different dimensionality using various chelating ligands: a) isolated [Mn_{10}] complex in **1**; b) 2D square network in **2**; c) 3D diamondoid network in **3**. Hydrogens, interstitial solvent molecules and anions are omitted for clarity. Atom colors: pink: Mn^{II}; green: Mn^{III}; blue: N; red: O; gray: C.

EXPERIMENTAL SECTION

General Procedures and Materials. All manipulations were carried out aerobic conditions using materials without any further purifications. *Caution! Perchlorate and azide salts are potentially explosive; such compounds should be synthesized and used in small quantities and should be treated with utmost care at all times.*

Synthesis. $[Mn^{III}_6Mn^{II}_4(L_1)_6(\mu_4\text{-}O)_4(\mu_3\text{-}N_3)_4(CH_3CN)_{11}(H_2O)]\cdot(ClO_4)_2\cdot(CH_3CN)_{8.5}$ (1). $Mn(ClO_4)_2\cdot 6H_2O$ (0.06 g, 0.16 mmol), 9*H*-fluorene-9,9-dimethanol (H_2L_1, 0.03 g, 0.13 mmol), and NaN_3 (0.01 g, 0.15 mmol) were dissolved in a mixture of CH_3OH (3 mL) and CH_3CN (12 mL). After 5 h stirring, the red-brown solution was filtered, and the filtrate was left undisturbed to evaporate. Red to red-brown block crystals were formed during the next 10 days. Yield: 32%. Elemental analysis (%) Calcd for $[Mn^{III}_6Mn^{II}_4(L_1)_6(\mu_4\text{-}O)_4(\mu_3\text{-}N_3)_4(CH_3CN)_{11}(H_2O)]\cdot(ClO_4)_2\cdot(CH_3CN)_{8.5}$ (1) ($C_{129}H_{132.5}Mn_{10}N_{31.5}O_{25}Cl_2$): C 49.27, H 4.25, N 14.03; found: C 48.93, H 4.57, N 14.85. Selected IR data (KBr pellet): $\bar{\nu}$ = 3426 (m), 3061 (m), 2901 (m), 2848 (m), 2304 (w), 2273 (w), 2050 (s), 1632 (m), 1476 (m), 1446 (m), 1380 (m), 1315 (m), 1226 (w), 1114 (s), 1080 (s), 1061 (s), 929 (m), 766 (m), 737 (s), 647 (s), 569 (m), 529 (s), 439 (w) cm^{-1}.

$[Mn^{III}_6Mn^{II}_4(L_2)_6(\mu_3\text{-}N_3)_4(\mu_4\text{-}O)_4(CH_3OH)_4(dca)_2]$ (2). A solution of NaN_3 (0.013 g, 0.2 mmol) in CH_3OH (2 mL) was added with stirring to a slurry of $Mn(ClO_4)_2\cdot 6H_2O$ (0.06 g, 0.16 mmol) and pentane-2,4-diol (H_2L_2, 0.06 g, 0.67 mmol, D/L and meso- isomers) in CH_3CN (10 mL). Sodium dicyanamide (0.02 g, 0.22 mmol) was added to the mixture that was then stirred for 1 h, light-brown solution was allowed to slowly evaporate. X-ray quality brown shuttle-like crystals of **2** were obtained in 1 week. Yield: 40%. Elemental analysis (%) Calcd for $[Mn^{III}_6Mn^{II}_4(L_2)_6(\mu_3\text{-}N_3)_4(\mu_4\text{-}O)_4(CH_3OH)_4(dca)_2]$ (2) ($C_{38}H_{88}Mn_{10}N_{18}O_{20}$): C 27.39, H 5.32, N 15.13; found: C 27.62, H 5.11, N 15.30. Selected IR data (KBr pellet): $\bar{\nu}$ = 3416 (w), 2970 (w), 2180 (s), 2058 (s), 1610 (m), 1310 (m), 1123 (m), 1090 (m), 936 (s), 651 (s) cm^{-1}.

Chart 1. 1,3-Propanediol Derivatives: a) 9*H*-Fluorene-9,9-dimethanol (H_2L_1); b) 2,4-Pentanediol (H_2L_2); c) 2-Methyl-2,4-pentanediol (H_2L_3)

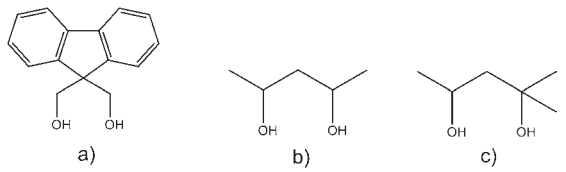

$[Mn^{III}_6Mn^{II}_4(L_3)_6(\mu_3\text{-}N_3)_4(\mu_4\text{-}O)_4(N_3)_2]\cdot(CH_3OH)_4$ (3). A solution of NaN_3 (0.13 g, 2 mmol) in CH_3OH (2 mL) was added with stirring to a slurry of $Mn(ClO_4)_2\cdot 6H_2O$ (0.72 g, 2 mmol), rac-2-methylpentane-2,4-diol (H_2L_3, 0.48 g, 4 mmol) in CH_3CN (20 mL). After the mixture had been stirred for ca. 5 min, the solution was left undisturbed in a closed vial. After ca. 5 days, small brown crystals of **3** were obtained in 80% yield. Dark-brown rhombic crystals of **3** suitable for X-ray crystal analysis were obtained after several days by layering of hexane on the resultant solution of the same reaction. Elemental analysis (%) Calcd for $[Mn^{III}_6Mn^{II}_4(L_3)_6(\mu_3\text{-}N_3)_4(\mu_4\text{-}O)_4(N_3)_2]\cdot(CH_3OH)_4$ (**3**) ($C_{40}H_{100}Mn_{10}N_{18}O_{20}$): C 28.22, H 5.92, N 14.81; found: C 28.08, H 6.01, N 14.77. Selected IR data (KBr pellet): $\bar{\nu}$ = 2970 (m), 2148 (m), 2058 (s), 1448 (m), 1310 (m), 1147 (m), 1041 (m), 928 (m), 659 (s) cm^{-1}.

Physical Measurements. Elemental analysis (C, H, and N) were carried out on a PerkinElmer 2400 Elemental Analysis. IR spectra were recorded in the range 400−4000 cm^{-1} on a Bruker IFS 66v/S IR spectrometer using KBr pellets. Magnetic measurements have been performed with a Quantum Design SQUID magnetometer MPMS-XL housed at the Centre de Recherche Paul Pascal at temperatures between 1.8 and 300 K and dc magnetic fields ranging from 0 to 7 T. Measurements were performed using polycrystalline samples of **1** (9.80 mg) that were filtered from their mother liquor and briefly dried in air (t < 2 min.). Measurements for **2** and **3** were reproducibly obtained for polycrystalline samples (7.49 and 12.30 mg) covered and thus restrained in a minimum of their frozen mother liquor within a sealed straw to prevent desolvation of the solid. No evaporation of the mother liquor was observed during the measurements. The mass of the sample was determined after the measurements and subsequent mother liquor evaporation. For these experiments, the magnetic data were corrected for the sample holder (plastic bag), mother liquor, and the diamagnetic contribution.

Crystallography. The crystal data for **1** were recorded on a Bruker APEX-II CCD system with Mo-Kα radiation (λ = 0.71069 Å) at 185 ± 2 K. The crystal structures were solved by means of direct methods and refined employing full-matrix least-squares on F^2 (*SHELXTL-97*).[7a] All non-hydrogen atoms were refined anisotropically except solvent acetonitrile molecules and perchlorate anions. Hydrogen atoms of the organic ligands were generated theoretically onto the specific atoms and refined isotropically with fixed thermal factors. Single-crystal structure determination of **2** and **3** were carried out on a Siemens SMART CCD diffractometer equipped with graphite-monochromated Mo Kα radiation (λ = 0.71073 Å) at 293 ± 2 K. Data processing was accomplished with the *SAINT* processing program.[7b] The structures were solved by direct methods and refined with the full-matrix least-squares technique using the program *SHELXTL-97*.[7a] Anisotropic thermal parameters were assigned to all non-hydrogen atoms.

DFT Calculations. All of the calculations have been performed with the *SIESTA* program (Spanish Initiative for Electronic Simulations with

Thousands of Atoms),[8a−c] using the GGA exchange-correlation functional proposed by Perdew, Burke, and Erzenhorf (PBE).[8d]

RESULTS AND DISCUSSION

Structure Description. The $[Mn^{III}_6Mn^{II}_4(L_1)_6(\mu_4\text{-}O)_4(\mu_3\text{-}N_3)_4]^{2+}$ core (Figures 1 and 2) in **1** is analogous to other $[Mn_{10}]$ complexes,[4a,b] that can be viewed as a supertetrahedron consisting of six $[Mn^{II}Mn^{III}Mn^{II}]L_1$ motifs connected by four sharing heptacoordinated Mn^{II} metal ions (part a of Figure 1 and Figure 2, Table 1 and Table S1 of the Supporting Information). The L_1 ligands are fully deprotonated and each coordinate with one Mn^{III} and two Mn^{II} ions in a $\eta^2:\eta^2:\mu_3$ mode to give the linear $[Mn^{II}Mn^{III}Mn^{II}]L_1$ unit (Figure 2). This trinuclear moiety has been isolated as an $S_T = 7$ SMM complex from *cis,cis*-1,3,5-cyclohexane-triol by E. Brechin et al.[11] Magnetic measurements and DFT calculations on related systems possessing the same $[Mn^{II}Mn^{III}Mn^{II}]$ motif confirm the recurrence of the ferromagnetic $Mn^{II}-Mn^{III}$ interactions in this unit.[3m,4,11,12] It is also interesting to note that the hexanuclear $[Mn^{III}_6O_4X_4]^{6+}$ (X = Cl^-, Br^-) complexes reported by D. Hendrickson and G. Christou,[13] have a face-capped octahedral Mn^{III} topology analogous to the one observed in **1** (Figure 2). These $[Mn^{III}_6O_4X_4]$ complexes exhibit an $S_T = 12$ spin ground state induced by the presence of ferromagnetic $Mn^{III}-Mn^{III}$ interactions. The structural comparisons of **1** with $[Mn_{10}]$-based systems[3m,4,12] and related geometrical $[Mn^{II}_2Mn^{III}]$ and $[Mn^{III}_6]$ structures[11,13] suggest that **1** should display an $S_T = 22$ ground spin state resulting from both $Mn^{II}\cdots Mn^{III}$ and $Mn^{III}\cdots Mn^{III}$ ferromagnetic interactions. It should be mentioned that no obvious intercomplex contacts has been found in the crystal packing justifying the fact that complexes in **1** can be considered

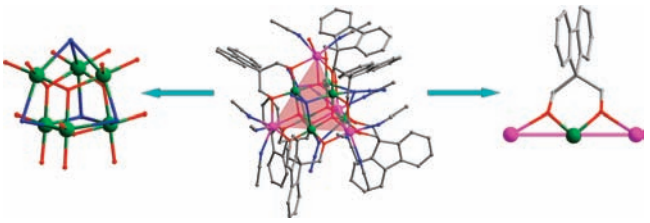

Figure 2. Structure of **1** (center) highlighting the inner $[Mn^{III}_6]$ core (left) and the linear trinuclear $[Mn^{II}-Mn^{III}-Mn^{II}]$ motif (right).

Table 1. Crystallographic Data for 1, 2, and 3, Respectively

	1	2	3
formula	$C_{129}H_{132.5}Cl_2Mn_{10}N_{31.5}O_{25}$	$C_{38}H_{88}Mn_{10}N_{18}O_{20}$	$C_{40}H_{100}Mn_{10}N_{18}O_{20}$
fw	3144.46	1654.57	1690.68
cryst. syst	triclinic	tetragonal	orthorhombic
space group	*P*-1	*P*-42$_1$*c*	*Pbcm*
a, (Å)	15.231(5)	14.0358(7)	13.745(3)
b, (Å)	15.988(5)	14.0358(7)	22.346(5)
c, (Å)	30.034(5)	16.4004(15)	22.592(5)
α, (deg)	92.271(5)	90	90
β, (deg)	91.599(5)	90	90
γ, (deg)	90.982(5)	90	90
V, (Å)^3	7304(4)	3230.9(4)	6939(2)
D_{Calcd}, (g cm^{-3})	1.430	1.701	1.618
Z	2	2	4
F(000)	3167	1680	3456
cryst size (mm)	0.23 × 0.24 × 0.26	0.27 × 0.23 × 0.18	0.17 × 0.14 × 0.12
temperature, K	185(2)	296(2)	293(2)
θ range for data collection (deg)	1.82 − 25.11	1.91 − 28.29	1.48 − 25.32
index range	$-17 \le h \le 18$	$-18 \le h \le 13$	$-16 \le h \le 15$
	$-19 \le k \le 18$	$-18 \le k \le 18$	$-26 \le k \le 25$
	$-35 \le l \le 35$	$-21 \le l \le 21$	$-27 \le l \le 25$
reflections collected	44 693 (R_{int} = 0.026)	22 846 (R_{int} = 0.073)	32 916 (R_{int} = 0.075)
independent reflections	25 752	3994	6297
observed reflections ($I > 2\sigma(I)$)	18 826	2455	3332
data, restrains, params	25752, 17, 1637	3994, 18, 188	6297, 6, 217
μ, (mm^{-1})	0.946	1.961	1.828
R_1 (observed)[a]	0.0683	0.0500	0.1081
wR_2 (observed)	0.2065[b]	0.1252[c]	0.3080[d]
S[e]	1.021	1.022	1.091
largest diff. peak, hole in e Å^{-3}	2.04, −1.89	0.52, −0.64	1.30, −1.20

[a] $R_1 = \Sigma\,||F_0| - |F_c||/\,\Sigma|F_0|$. [b] $wR_2 = [\Sigma w(F_0^2 - F_c^2)^2/\Sigma w(F_0^2)^2]^{1/2}$; $w = 1/[S^2F_0^2 + (0.0996P)^2 + 31.2037P]$; where $P = (F_0^2+2F_c^2)/3$. [c] $wR_2 = [\Sigma w(F_0^2 - F_c^2)^2/\Sigma w(F_0^2)^2]^{1/2}$; $w = 1/[S^2F_0^2 + (0.0754P)^2 + 1.3699P]$; where $P = (F_0^2+2F_c^2)/3$. [d] $wR_2 = [\Sigma w(F_0^2 - F_c^2)^2/\Sigma w(F_0^2)^2]^{1/2}$; $w = 1/[S^2F_0^2 + (0.2000P)^2 + 0.0000P]$; where $P = (F_0^2+2F_c^2)/3$. [e] Goodness-of-Fit: $S = [\Sigma w(F_0^2 - F_c^2)^2/(n-p)]^{1/2}$, where *n* is the number of reflections and *p* is the number of parameters.

dx.doi.org/10.1021/ic201154n |*Inorg. Chem.* 2011, 50, 8580–8587

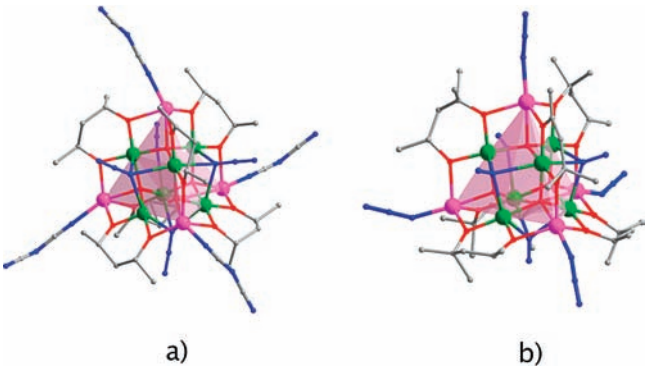

Figure 3. $[Mn_{10}]$ core structures in **2** (a) and in **3** (b).

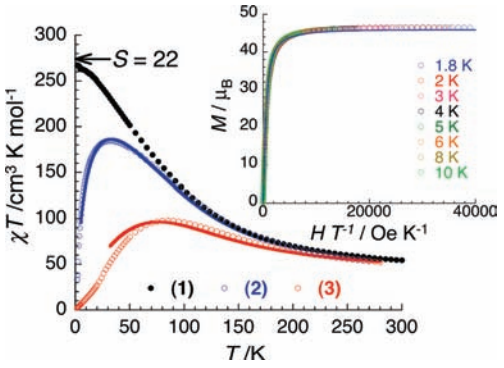

Figure 4. χT vs T data for **1**, **2** and **3** (with χ defined as the molar magnetic susceptibility and equal to (i) M/H measured at H = 1000 Oe from 300 to 20 K and (ii) χ'_{ac} at H_{dc} = 0 Oe, ν_{ac} = 100 Hz, H_{ac} = 3 Oe from 20 to 1.8 K).[15] Solid lines are the best fit of the data using a mean field approach described in the text. Insert: M vs H/T data for **1**. Solid line is the best fit of the data using an S = 22 Brillouin function.

as a well-isolated on a structural and probably magnetic point of views.

Introduction of linkers to connect this $[Mn_{10}]$ building-block into networks failed due to the steric hindrance caused by the fluorene part of the L_1 ligand. Therefore, a natural extension of this work was to use less bulky 1,3-propanediol derivatives combined with ditopic linkers. This synthetic approach with 2,4-pentanediol (H_2L_2) and 2-methyl-2,4-pentanediol (H_2L_3) ligands is illustrated by the synthesis of **2** and **3**.

The crystal structure of **3** (part c of Figure 1 and part b of Figure 3, Table 1 and Table S3 of the Supporting Information)[10] reveals a covalently bonded 3D structure composed of $[Mn^{III}_6Mn^{II}_4(L_3)_6(\mu_4\text{-}O)_4(\mu_3\text{-}N_3)_4]^{2+}$ repeating motif, connected to four neighboring $[Mn_{10}]$ through four end-end (EE) azido bridges. The rigid and quasi-linear N_3^- anions (N−N−N: 173.3 and 180.0°) occupy the supertetrahedron corners generating an open 4-connected diamondoid network (part c of Figure 1 and part b of Figure 3), which is the most favorable architecture from tetrahedral coordinating building blocks like adamantine.[14] As expected, the dialcohol ligand (H_2L_3) is fully deprotonated and coordinates with two Mn^{II} and one Mn^{III} ions a $\eta^2:\eta^2:\mu_3$ mode to give the linear $[Mn^{II}Mn^{III}Mn^{II}]L_3$ moiety. Like in **1**, six of these trinuclear subunits are assembled together by sharing Mn^{II} metal ions, four μ_4-O and four end-on (EO) μ_3-N_3 to give the $[Mn_{10}]$ supertetrahetral moiety. The four Mn^{II} ions adopt a trigonal−bipyramidal coordination sphere occupied by three μ-O from the L_3^{2-} ligands, one central μ_4-O^{2-}, and one EE azide anion. It should be emphasized that the N_3^- anions play an important role for the formation of both (i) the $[Mn_{10}]$ building unit by connecting three Mn^{III} ions in an EO mode and thus stabilizing the faces of the $[Mn_{10}]$ supertetrahedral complex; and (ii) the 3D coordination network by EE azide anions that connect Mn^{II} metal ions between neighboring $[Mn_{10}]$.

The direct replacement of the EE azide bridges by organic linkers was unsuccessful using the H_2L_3 ligand. However when pentane-2,4-diol (H_2L_2, Chart 1) is used and dca^- (dicyanamide) introduced as $[Mn_{10}]$ linker, the $[Mn^{III}_6Mn^{II}_4(L_3)_6(\mu_3\text{-}N_3)_4(\mu_4\text{-}O)_4(CH_3OH)_4(dca)_2]$ (**2**) (Table 1 and Table S2 of the Supporting Information)[10] compound is isolated. X-ray diffraction study (Table 1) reveals that the $[Mn_{10}]$ building unit observed in **1** and **3** is also present in **2** and are bridged by μ-1,5-dicyanamide anions to form a 2D network (part b of Figure 1 and part a of Figure 3). As already observed between **1** and **3** (Tables S1 and S3 of the Supporting Information),[10] the supertetrahedral $[Mn_{10}]$ moiety is only slightly geometrically modified in **2** at the Mn^{II} vertex (part a of Figure 3 and Table S2 of the Supporting Information)[10] that is heptacoordinated in **1**, pentacoordinated in **3**, and becomes hexacoordinated in **2** (Figures 1, 2, and 3). Rather than the diamondoid arrangement described for **3**, **2** exhibits a 2D square lattice of $[Mn_{10}]$ thanks to the flexibility and nonlinearity of the dca^- bridge. As expected on the basis of the relative length of the anionic linkers, intercomplex $Mn^{II}\cdots Mn^{II}$ distances in **2** are significantly larger, 8.082 Å, than for **3** (6.001 Å and 6.219 Å).

Magnetic Properties. The magnetic properties of the three $[Mn_{10}]$-based materials have been studied in great detail. As expected, the χT product at 280 K normalized per $[Mn_{10}]$ unit is nearly identical for the three samples at 55.7, 51.7, 52.2 cm^3 K/mol for **1**, **2**, and **3**, respectively. Lowering the temperature, the χT values increase (Figure 4, and Figures S1−S3 of the Supporting Information) toward maximum values of 267, 184, and 98 cm^3 K/mol at 1.8, 31, and 83 K respectively indicating dominant ferromagnetic interactions within the $[Mn_{10}]$ core as already observed in related systems.[3m,4,12] The spin content of the materials can be estimated by fitting the experimental data with a Curie−Weiss law above 150 K. This qualitative approach leads to Curie constants of 40.1, 37.6, and 39.1 cm^3 K/mol, for **1**, **2**, and **3** respectively, in good agreement with the presence of six Mn^{III} (S = 2, $g \approx 2$) and four Mn^{II} ($S = {}^5/_2$, $g \approx 2$) metal ions.[16]

Below 31 and 83 K for **2** and **3**, the χT product in Figure 4 decreases to 33.2 and 1.9 cm^3 K/mol at 1.8 K indicating the presence of antiferromagnetic interactions likely between $[Mn_{10}]$ unit through dicyanamide and azide bridges respectively. As expected from the structure analysis of **1** (vide supra), the absence of χT product decrease down to 1.8 K confirms the remarkably good magnetic isolation of the $[Mn_{10}]$ moieties in the crystal structure, whereas, in analogous $[Mn_{10}]$ complexes,[4a,b] the presence of intercomplex antiferromagnetic interactions have been detected above 1.8 K. The S_T = 22 spin ground state of **1** is confirmed by the χT product reached at 1.8 K: 267 cm^3 K/mol (expected 274 cm^3 K/mol with g = 2.08, Figure 4), and the M versus H/T data below 10 K that fit very well to an S = 22 Brillouin function (with g = 2.08(2), as seen in the insert of Figure 4 and in Figure S4 of the Supporting Information). Therefore, as expected based on related high-spin $[Mn_{10}]$-based systems,[3m,4,12] the intracomplex interactions present in the $[Mn^{III}_6Mn^{II}_4]$ core are all ferromagnetic by nature as also confirmed by the DFT calculations reported below.

dx.doi.org/10.1021/ic201154n |*Inorg. Chem.* 2011, 50, 8580–8587

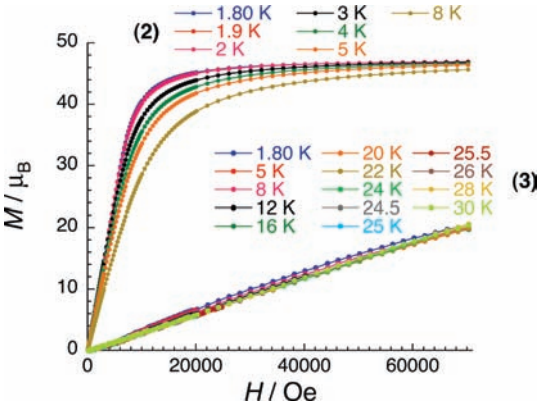

Figure 5. M vs H data for **2** and **3** at different temperatures. Solid lines are guides.

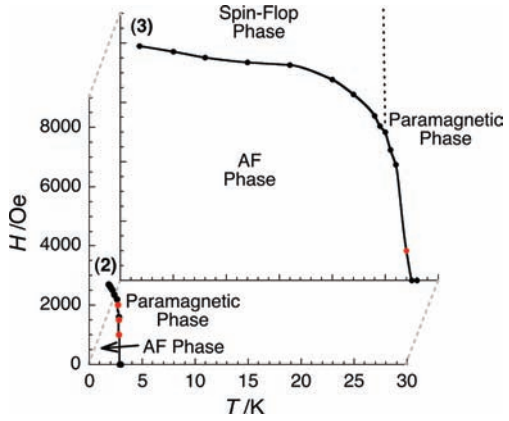

Figure 6. (T, H) phase diagrams for **2** and **3**. Black dots: Location of the maximum of susceptibility from dM/dH vs H data (Figures S6 and S8 of the Supporting Information); Red dots: Location of the maximum of susceptibility from χ vs T data (Supporting Information). The solid lines are guides.

Using the experimental χT versus T data of **1**, the average intercomplex magnetic interactions in **2** and **3** have been estimated in the frame of the mean-field approximation.[17] Relatively good simulations of the χT versus T data for **2** and **3** have been obtained with $zJ'/k_B = -0.025(5)$ K and $-0.24(4)$ K (with $g = 2$) that correspond to $Mn^{II}\cdots Mn^{II}$ magnetic interactions of $-0.5(1)$ K and $-4.6(8)$ K (with $z = 4$) through dca^- and N_3^- bridges.[18] These interaction estimations fall quite well in the range of the values determined on related Mn^{II}/dca^- (-0.05 to -1.5 K) and Mn^{II}/N_3^- (-1.5 to -8 K) systems.[19,20]

At 1.8 K, M versus H data for **2** and **3** shown in Figure 5 and in Figures S6 and S8 of the Supporting Information exhibits an inflection point at H_C around 2700 and 7900 Oe (seen also by the maximum of the dM/dH versus H data).

Using combined M versus H and χ versus T data, it has been possible to follow the temperature dependence of this characteristic field, H_C, (Figure 6) that extrapolates to zero at $T_N = 2.9$ and 27.5 K for **2** and **3**, respectively. The resulting phase diagrams shown in Figure 6 demonstrate the stabilization of an ordered antiferromagnetic ground state in **2** and **3** below T_N induced by the inter-$[Mn_{10}]$ interactions through dca^- and N_3^- bridges. Nevertheless below T_N, the field induced magnetic behavior in these two compounds is different. Whereas the magnetization in **2** saturates rapidly above H_C (around 47 μ_B, like **1**) as expected for a metamagnetic behavior (with a field induced antiferromagnetic/paramagnetic phase transition), the magnetization for **3** is increasing very slowly with the applied dc magnetic field and is very far from saturation even at 1.8 K and 7 T (around 20.5 μ_B). Therefore, **3** displays an antiferromagnetic behavior with $H_C = H_{C1}$ corresponding to an antiferromagnetic/spin-flop phase transition.

For the phase diagram of **2**, the intercomplex interactions can be estimated at $zJ'/k_B \approx -0.01$ K based on the extrapolation of the critical field at $T = 0$ K (3200 Oe) and the well established relation for metamagnetic systems between H_C and zJ': $g\mu_B H_C(0)S_T = -2zJ'S_T^2$.[21] In the case of **3**, the estimation of zJ' from the critical fields is more complicated. H_{C2} corresponding to the antiferromagnetic/paramagnetic phase transition is not accessible in the experimental window of dc fields. Nevertheless neglecting the anisotropy contribution on H_{C2} ($|zJ'| \gg |D|$), this field can be deduced from the perpendicular susceptibility, $\chi_{perp} = 1.6$ cm^3/mol, obtained experimentally by the slope of the M(1.8 K) versus H data at low field: $H_{C2} \approx Ng\mu_B S_T/\chi_{perp} \approx 16$ T. The intercomplex interactions are then estimated in **3** at $zJ'/k_B \approx -0.25$ K from the $g\mu_B H_{C2}S_T \approx -4zJ'S_T^2$ relation.[21] It is worth mentioning that the zJ' value obtained from the χT versus T data (vide supra) is in perfect agreement for **3** with the one estimated from H_{C2} but is obviously overestimated for **2** in comparison to the value deduced from H_C.

The magnetic anisotropy of the $S_T = 22$ $[Mn_{10}]$ complex can also be estimated from antiferromagnetic/spin-flop critical field, H_{C1}, observed for **3**. Solving the following second order equation: $(g\mu_B H_{C1}S_T)^2 = 4|D|S_T^2(2|zJ'|S_T^2 - |D|S_T^2)$ with $H_{C1} = 8000$ Oe and $zJ'/k_B \approx -0.25$ K,[21] the $|D|$ parameter is roughly estimated at about 1.3 mK (justifying the above $|zJ'| \gg |D|$ approximation). It is worth noting that this D value is comparable to the estimation made by O. Waldman et al. on the $S_T = 83/2$ $[Mn_{19}]$ complex.[22]

Details of DFT Calculations. Unfortunately, as in related complexes,[3m,4,12] the individual intracomplex magnetic interactions are impossible to evaluate from experimental χT versus T data due to the core geometry and the number of both spin carrier and magnetic interaction of the $[Mn_{10}]$ unit. Therefore, numerical DFT calculations (Siesta code) using the PBE functional have been performed for the three compounds.[23] On the basis of the structural data, the geometry of the different magnetic interaction pathways has been compared to simplify the calculations without loosing the physical meaning of the used models (the Hamiltonians, geometrical parameters and calculated intra-$[Mn_{10}]$ interactions are given Figure 7 and Tables S4−S6 of the Supporting Information). The values of 50 meV for the energy shift and 250 Ry for mesh cutoff provide a good compromise between accuracy and computer time to estimate exchange coupling constants. For **1** and **2**, seven calculations have been performed: a high-spin solution ($S = 22$), an $S = 2$ configuration with negative spin at all the Mn^{II} cations {Mn1, Mn2, Mn3, Mn4}, an $S = 6$ configuration with negative spin at Mn^{III} cations {Mn5, Mn6, Mn9, Mn10}, an $S = 7$ configuration with negative spin at Mn^{II} cations {Mn2, Mn3, Mn4}, an $S = 8$ configuration with negative spin at {Mn1, Mn2, Mn8} and two $S = 9$ configurations with negative spin at {Mn2, Mn8, Mn10} and {Mn2, Mn6, Mn7}. For **3**, five calculations have been performed: a high-spin solution ($S = 22$), an $S = 2$ configuration with negative spin at all of the Mn^{II} cations {Mn1, Mn2, Mn3, Mn4}, an $S = 6$ configuration with negative spin at Mn^{III} cations {Mn6,

dx.doi.org/10.1021/ic201154n |Inorg. Chem. 2011, 50, 8580–8587

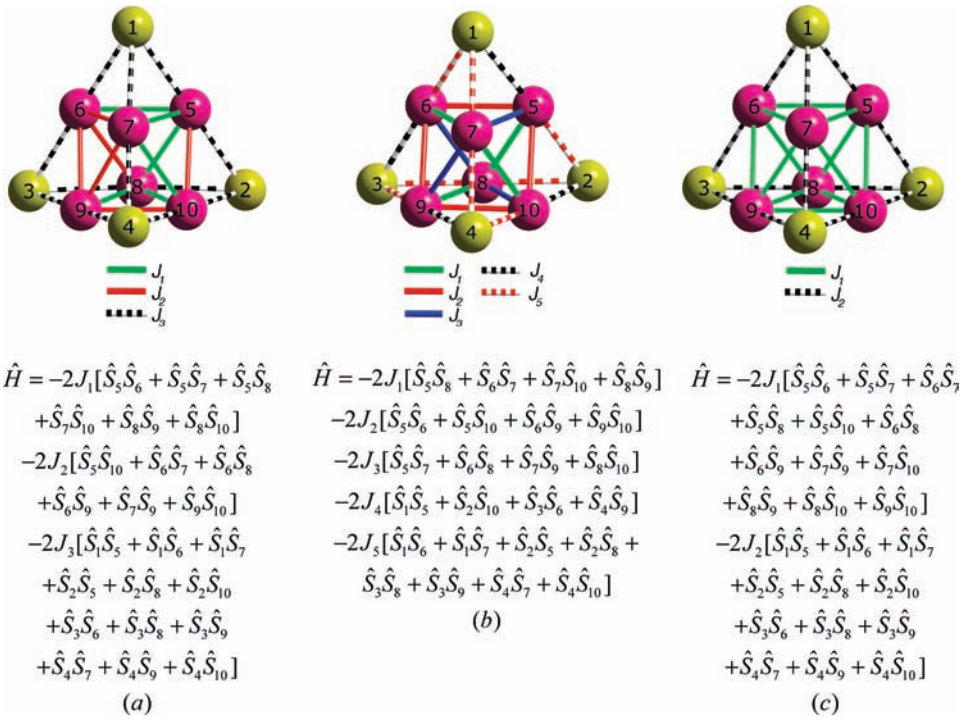

Figure 7. Topology of the exchange interactions in the three studied compounds: a) **1**, b) **2**, c) **3**; with the corresponding spin Hamiltonian. The plain and dotted bonds represent $Mn^{III}-Mn^{III}$ and $Mn^{III}-Mn^{II}$ interactions respectively.

Mn7, Mn8, Mn10}, and two $S = 14$ configurations with negative spin at {Mn7, Mn8} and {Mn5, Mn6}.

This DFT approach (Tables S4−S6 of the Supporting Information) allows us to confirm the ferromagnetic nature of all of the magnetic interactions within the $[Mn_{10}]$ core in **1**, **2**, and **3** and thus its $S_T = 22$ ground state. Systematically among this series of compounds, the $Mn^{III}\cdots Mn^{III}$ interactions through μ_4-oxido/μ_3-1,1,1-azido bridges are larger than $Mn^{II}\cdots Mn^{III}$ ones via μ_4-oxido/μ-alkoxido bridges (Tables S4−S6 of the Supporting Information). It is also clear from the DFT calculations that the $Mn^{III}\cdots Mn^{III}$ interaction increases with the decrease of both $Mn^{III}-Mn^{III}$ distance and $Mn^{III}-X-Mn^{III}$ angle. It should be noted that this trend and also similar $Mn^{III}\cdots Mn^{III}$ interaction values were observed for the related $[Mn_{19}]$ complex made of two fused $[Mn_{10}]$ supertetrahedron sharing a Mn^{II} vertex.[12] In the case of the $Mn^{II}\cdots Mn^{III}$ exchange interaction, the same tendency is observed, that is a decrease of both $Mn^{II}-Mn^{III}$ distance and $Mn^{II}-O-Mn^{III}$ angle promotes the ferromagnetic interactions independently of the Mn^{II} coordination sphere. This result is in line with that was observed in an analogous $[Mn_{10}]$ complex obtained by G. Christou et al.,[4a] that shows weaker $Mn^{II}\cdots Mn^{III}$ ferromagnetic interactions because of the larger $Mn^{II}-O-Mn^{III}$ angles and longer $Mn^{II}-Mn^{III}$ distances.

The $Mn^{II}\cdots Mn^{II}$ interactions between the $[Mn_{10}]$ supertetrahedron through *μ-1,3*-azido and *μ-1,5*-dicyanamide bridging ligands, has also been evaluated by DFT calculations and found to be antiferromagnetic in agreement with the magnetic measurements. The intercomplex magnetic interactions were estimated for the 3D network (**3**) using the whole unit cell (665 atoms) increasing the number of k-points to ensure the convergence. For the 2D network (**2**) the number of the atoms to consider in the unit cell is very large for a periodic calculation, hence the intermolecular exchange interaction has been calculated using only two units of the manganese supertetrahedron because it does not drastically affect the calculated values. Two solutions, a high-spin $S = 44$, and an $S = 0$ configuration, where all of the atoms of manganese of one supertetrahedron are aligned antiparallely to the other supertetrahedron, have been considered. In both compounds, the $Mn^{II}\cdots Mn^{II}$ intermolecular distance is relatively large around 8.082 Å in **2** and 6.001/6.219 Å in **3** but the $Mn^{II}\cdots Mn^{II}$ intercomplex interaction through dca^- and N_3^- stays significant as suggested by the experimental estimation of J'. For **2**, these exchange couplings have been evaluated by DFT at about −0.7 K in good agreement with the magnetic measurements (vide supra). In the case of **3**, the two different intermolecular interactions have been estimated at −11.5 and −24.5 K. These values are significantly larger than the average experimental one (−4.6 K). To test if this overestimation is general for $Mn^{II}\cdots Mn^{II}$ intercomplex interactions through single N_3^- bridge, DFT calculations have been performed on a known dinuclear Mn(II) complex (CSD refcode RASJAX) that displays experimentally an intramolecular coupling of −1.65 K.[24a] The calculated J value using Siesta code, that is employing the same methodology than for the $[Mn_{10}]$ systems, is also overestimated at −13.6 K. To check the influence of the functional and the basis set, the calculations have been repeated using *Gaussian09*,[24b] a B3LYP functional,[24c] and TZV basis[24d] sets leading to a value of −10.1 K that is still above the experimental value. Thus, the use of a hybrid functional reduces significantly the estimation of the J value, but stays overestimated.

CONCLUDING REMARKS

In summary, the synthesis of new magnetic materials based on high-spin complexes such as the $S_T = 22$ $[Mn_{10}]$ supertetrahedron complex is a great challenge in coordination chemistry and molecular magnetism. Our synthetic strategy using 1,3-propanediol

dx.doi.org/10.1021/ic201154n |*Inorg. Chem.* 2011, 50, 8580–8587

derivatives together with azide and dicyanamide bridging ligands has been successful with the isolation of the first 2D and 3D networks of $[Mn_{10}]$ building-blocks. In the reported synthetic conditions, the stability of the $[Mn_{10}]$ complex is remarkably good that allows us to imagine many new materials combining these high-spin moieties and other diamagnetic but also paramagnetic linkers to design for example ordered magnets. However, the assemblage of the $[Mn_{10}]$ motifs into large aggregates with high-spin ground state should be explored by a fine modification of the 1,3-propanediol ligand. Multifunctional materials could also be obtained combining the properties of the linker or the diol ligand with those of the high-spin unit. For example using chiral dialcohol ligands like (*R*)-2-methyl-2,4-pentanediol results chiral 3D networks ($P2_12_12$) of $[Mn_{10}]$ units analogous of **3**. Work is in progress to investigate the magnetochiral properties of this system.

■ ASSOCIATED CONTENT

Supporting Information. Additional magnetic data, computational details of DFT calculations, selected bond distances and angles tables, as well as X-ray crystallographic files in CIF format for the reported compound. This material is available free of charge via the Internet at http://pubs.acs.org. X-ray crystallographic files of **1**−**3** can also be obtained free of charge from The Cambridge Crystallographic Data Centre with CCDC 810781, 798924, and 798923 (**1**, **2**, and **3**, respectively) via www.ccdc.cam.ac.uk/data_request/cif.

■ AUTHOR INFORMATION

Corresponding Author

*Tel: (+86) 431-8516-8331; Fax: (+86) 431-8516-8331; E-mail: wug@jlu.edu.cn (G.W.), sqiu@jlu.edu.cn (S.Q.).
*Tel: (+33) 5 56 84 56 50; Fax: (+33) 5 56 84 56 00; E-mail: clerac@crpp-bordeaux.cnrs.fr (R.C.).

■ ACKNOWLEDGMENT

The authors thank National Natural Science Foundation of China (grant No. 20901027), the Natural Science Foundation of Jilin Province (grant No. 20080121), "111" project (B07016), the University of Bordeaux, ANR (NT09_469563, AC-MAGnets project), Région Aquitaine, GIS Advanced Materials in Aquitaine (COMET Project), CNRS, the *Ministerio de Ciencia e Innovación* and *Generalitat de Catalunya* through grants CTQ2008-06670-C02-01 and 2009SGR-1459 respectively for financial support. The authors thankfully acknowledge the computer resources, technical expertise and assistance provided by the Barcelona Supercomputing Center (*Centro Nacional de Supercomputación*). E.C. thanks to the *Ministerio de Ciencia e Innovación* for his Ph.D. grant.

■ REFERENCES

(1) (a) Christou, G.; Gatteschi, D.; Hendrickson, D. N.; Sessoli, R. *MRS Bull.* **2000**, *25*, 66. (b) Gatteshi, D.; Sessoli, R. *Angew. Chem., Int. Ed.* **2003**, *42*, 268. (c) Leuenberger, M.; Loss, D. *Nature* **2001**, *410*, 789. (d) Aromi, G.; Brechin, E. K. *Struct. Bonding (Berlin)* **2006**, *122*, 1.

(2) (a) Wernsdorfer, W.; Aliaga-Alcalde, N.; Hendrickson, D. N.; Christou, G. *Nature* **2002**, *416*, 406. (b) Tiron, R.; Wernsdorfer, W.; Aliaga-Alcalde, N.; Christou, G. *Phys. Rev. B* **2003**, *68*, 140407(R). (c) Tiron, R.; Wernsdorfer, W.; Foguet-Albiol, D.; Aliaga-Alcalde, N.; Christou, G. *Phys. Rev. Lett.* **2003**, *91*, 227203.

(3) (a) Miyasaka, H.; Nakata, K.; Sugiura, K.; Yamashita, M.; Clérac, R. *Angew. Chem., Int. Ed.* **2004**, *43*, 707. (b) Yoo, J.; Wernsdorfer, W.; Yang, E.-C.; Nakano, M.; Rheingold, A. L.; Hendrickson, D. N. *Inorg. Chem.* **2005**, *44*, 3377. (c) Miyasaka, H.; Nakata, K.; Lecren, L.; Coulon, C.; Nakazawa, Y.; Fujisaki, T.; Sugiura, K.; Yamashita, M.; Clérac, R. *J. Am. Chem. Soc.* **2006**, *128*, 3770. (d) Andruh, M. *Chem. Commun.* **2007**, 2565. (e) Lecren, L.; Wernsdorfer, W.; Li, Y.-G.; Vindigni, A.; Miyasaka, H.; Clérac, R. *J. Am. Chem. Soc.* **2007**, *129*, 5045. (f) Xu, H.-B.; Wang, B.-W.; Pan, F.; Wang, Z.-M.; Gao, S. *Angew. Chem., Int. Ed.* **2007**, *46*, 7388. (g) Roubeau, O.; Clérac, R. *Eur. J. Inorg. Chem.* **2008**, 4325. (h) Bai, Y.-L.; Tao, J.; Wernsdorfer, W.; Sato, O.; Huang, R.-B.; Zheng, L.-S. *J. Am. Chem. Soc.* **2006**, *128*, 16428. (i) Liu, C.-M.; Zhang, D.-Q.; Zhu, D.-B. *Inorg. Chem.* **2009**, *48*, 4980. (j) Song, X.; Yang, P.; Mei, X.; Li, L.; Liao, D. *Eur. J. Inorg. Chem.* **2010**, 1689. (k) Jones, L. F.; Prescimone, A.; Evangelisti, M.; Brechin, E. K. *Chem. Commun.* **2009**, *15*, 2023. (l) Yang, C.-I.; Tsai, Y.-J.; Hung, S.-P.; Tsai, H.-L.; Nakano, M. *Chem. Commun.* **2010**, *46*, 5716. (m) Moushi, E. E.; Stamatatos, T. C.; Wernsdorfer, W.; Nastopoulos, V.; Christou, G.; Tasiopoulos, A. J. *Inorg. Chem.* **2009**, *48*, 5049. (n) Lin, P.-H.; Burchell, T. J.; Clérac, R.; Murugesu, M. *Angew. Chem., Int. Ed.* **2008**, *47*, 8848.

(4) (a) Stamatatos, T. C.; Abboud, K. A.; Wernsdorfer, W.; Christou, G. *Angew. Chem., Int. Ed.* **2006**, *45*, 4134. (b) Manoli, M.; Johnstone, R. D. L.; Parsons, S.; Murrie, M.; Affronte, M.; Evangelisti, M.; Brechin, E. K. *Angew. Chem., Int. Ed.* **2007**, *46*, 4456. (c) Ako, A. M.; Hewitt, I. J.; Mereacre, V.; Clérac, R.; Wernsdorfer, W.; Anson, C. E.; Powell, A. K. *Angew. Chem., Int. Ed.* **2006**, *45*, 4926. (d) Nayak, S.; Beltran, L. M. C.; Lan, Y.; Clérac, R.; Hearns, N. G. R.; Wernsdorfer, W.; Anson, C. E.; Powell, A. K. *Dalton Trans.* **2009**, 1901. (e) Cremades, E.; Ruiz, E. *Inorg. Chem.* **2010**, *49*, 9641.

(5) (a) Hill, C. L. *Chem. Rev.* **1998**, *98*, 1.(b) Pope, M. T.; Müller, A. *Polyoxometalate Chemistry from Topology via Self-Assembly to Applications*; Kluwer Academic Publishers: The Netherlands, 2001. (c) Feng, P.; Bu, X.; Zheng, N. *Acc. Chem. Res.* **2005**, *38*, 293. (d) Dehnen, S.; Melullis, M. *Coord. Chem. Rev.* **2007**, *251*, 1259. (e) Osterloh, F. E. *Chem. Mater.* **2008**, *20*, 35. (f) Anson, C. E.; Eichöhfer, A.; Issac, I.; Fenske, D.; Fuhr, O.; Sevillano, P.; Persau, C.; Stalke, D.; Zhang, J. *Angew. Chem., Int. Ed.* **2008**, *47*, 1326. (g) Long, D.-L.; Tsunashima, R.; Cronin, L. *Angew. Chem., Int. Ed.* **2010**, *49*, 1736. (h) Vaqueiro, P. *Dalton. Trans.* **2010**, *39*, 5965.

(6) (a) Shaw, R.; Tidmarsh, I. S.; Laye, R. H.; Breeze, B.; Helliwell, M.; Brechin, E. K.; Heath, S. L.; Murrie, M.; Ochsenbein, S.; Güdel, H.-U.; McInnes, E. J. L. *Chem. Commun.* **2004**, 1418. (b) Brechin, E. K. *Chem. Commun.* **2005**, 514. (c) Collison, D.; McInnes, E. J. L.; Brechin, E. K. *Eur. J. Inorg. Chem.* **2006**, 2725. (d) Chaudhuri, P.; Kataev, V.; Büchner, B.; Klauss, H.-H.; Kersting, B.; Meyer, F. *Coord. Chem. Rev.* **2009**, *253*, 2261.

(7) (a) Sheldrick, G. M. *SHELX-97. Programs for Crystal Structure Solution and Refinement*; University of Göttingen: Germany, 1997. (b) Software packages *SMART*, and *SAINT*; Siemens Analytical X-ray Instruments Inc.: Madison, WI, 1996.

(8) (a) Artacho, E.; Gale, J. D.; García, A.; Junquera, J.; Martin, R. M.; Ordejón, P.; Sánchez-Portal, D.; Soler, J. M. *Siesta* 2006. (b) Soler, J. M.; Artacho, E.; Gale, J. D.; García, A.; Junquera, J.; Ordejón, P.; Sánchez-Portal, D. *J. Phys.: Condens. Matter* **2002**, *14*, 2745. (c) Artacho, E.; Sánchez-Portal, D.; Ordejón, P.; García, A.; Soler, J. M. *Phys. Status Solidi A* **1999**, *215*, 809. (d) Perdew, J.; Burke, K.; Ernzerhof, M. *Phys. Rev. Lett.* **1996**, *77*, 3865.

(9) The big family of 1,3-propanediol derivatives that have been used to produce numerous polynuclear Mn compounds. See refs 4d and 4e and (a) Moushi, E. E.; Stamatatos, T. C.; Wernsdorfer, W.; Nastopoulos, V.; Christou, G.; Tasiopoulos, A. J. *Angew. Chem., Int. Ed.* **2006**, *45*, 7722. (b) Moushi, E. E.; Lampropoulos, C.; Wernsdorfer, W.; Nastopoulos, V.; Christou, G.; Tasiopoulos, A. J. *Inorg. Chem.* **2007**, *46*, 3795. (c) Moushi, E. E.; Masello, A.; Wernsdorfer, W.; Nastopoulos, V.; Christou, G.; Tasiopoulos, A. J. *Dalton Trans.* **2010**, *39*, 4978.

(10) See the Supporting Information.

(11) Scott, R. T. W.; Parsons, S.; Murugesu, M.; Wernsdorfer, W.; Christou, G.; Brechin, E. K. *Chem. Commun.* **2005**, 2083.

(12) Ruiz, E.; Cauchy, T.; Cano, J.; Costa, R.; Tercero, J.; Alvarez, S. *J. Am. Chem. Soc.* **2008**, *130*, 7420.

(13) Aromi, G.; Knapp, M. J.; Claude, J.-P.; Huffman, J. C.; Hendrickson, D. N.; Christou, G. *J. Am. Chem. Soc.* **1999**, *121*, 5489.

(14) (a) Copp, S. B.; Subramanian, S.; Zaworotko, M. J. *J. Chem. Soc. Chem. Commun.* **1993**, 1078. (b) Hirsch, K. A.; Venkataraman, D.; Wilson, S. R.; Moore, J. S.; Lee, S. *J. Chem. Soc. Chem. Commun.* **1995**, 2199. (c) Carlucci, L.; Ciani, G.; Proserpio, D. M.; Rizzato, S. *Eur. J. Chem.* **2002**, *8* (7), 1519. (d) Wang, Z.; Zhang, B.; Fujiwara, H.; Kobayashi, H.; Kurmoo, M. *Chem. Commun.* **2004**, 416.

(15) It is worth mentioning that M/H (at 1000 Oe) and χ'_{ac}(0 Oe) are rigorously identical for compounds **2** and **3** below 30 K. In **1**, field effects are responsible for the difference between M/H (at 1000 Oe) and χ'_{ac}(0 Oe); See Figures S1−S8 of the Supporting Information.

(16) The deduced Weiss constants, +83, +87, and +77 K for **1**, **2**, and **3** respectively give only a confirmation of overall dominating ferromagnetic interactions in these systems.

(17) To take into account the interactions between $[Mn_{10}]$ complexes in **2** and **3**, the following definition of the susceptibility has been used (with the following definition of J': $H = -2J'\Sigma S_i S_{i+1}$):

$$\chi = \frac{\chi_{(1)}}{1 - \frac{2zJ'}{Ng^2\mu_B^2}\chi_{(1)}}$$

Note that $\chi_{(1)}$ is the experimental susceptibility of **1**. See for example: (a) Myers, B. E.; Berger, L.; Friedberg, S. *J. Appl. Phys.* **1969**, *40*, 1149. (b) O'Connor, C. J. *Prog. Inorg. Chem.* **1982**, *29*, 203.

(18) From J' (the mean-field estimation of the average interaction between $[Mn_{10}]$ units), the magnetic interaction between Mn(II) metal ions can be easily estimated at $J_{Mn\text{-}Mn} = J'S_T{}^2/S_{Mn}{}^2$ (with $S_T = 22$).

(19) (a) Zhang, Y. L.; Ling, Y.; Hu, A.-X.; Yao, T.- T.; Li, J. *Inorg. Chim. Acta* **2009**, *362*, 4867. (b) Bhar, K.; Khan, S.; Das, S.; Mitra, P.; Rosair, G.; Ribas, J.; Ghosh, B. K. *Inorg. Chim. Acta* **2010**, *363*, 3308.

(20) (a) Escuer, A.; Vicente, R.; Goher, M. A. S.; Mautner, F. A. *Inorg. Chem.* **1996**, *35*, 6386. (b) Song, X.; Xu, Y.; Li, L.; Jiang, Z.; Liao, D. *Inorg. Chem. Commun.* **2006**, *9*, 1212. (c) Ma, Y.; Cheng, A.-L.; Sun, W.-W.; Zhang, J.-Y.; Gao, E.-Q. *Inorg. Chem. Commun.* **2009**, *12*, 412.

(21) de Jongh, L. J.; Miedema, A. R. *Adv. Phys.* **1974**, *23*, 1.

(22) Waldman, O.; Ako, A. M.; Güdel, H. U.; Powell, A. K. *Inorg. Chem.* **2008**, *47*, 3486.

(23) (a) Soler, J. M.; Artacho, E.; Gale, J. D.; García, A.; Junquera, J.; Ordejón, P.; Sánchez-Portal, D. *J. Phys.: Condens. Matter* **2002**, *14*, 2745. (b) Perdew, J.; Burke, K.; Ernzerhof, M. *Phys. Rev. Lett.* **1996**, *77*, 3865.

(24) (a) Complex 6 in: Ni, Z.-H.; Kou, H.-Z.; Zheng, L.; Zhao, Y.-H.; Zhang, L.-F.; Wang, R.-J.; Cui, A.-L.; Sato, O. *Inorg. Chem.* **2005**, *44*, 4728. Note that the J value is given with the definition of the spin Hamiltonian used in this paper: $H = -2JS_1S_2$. (b) Frisch, M. J. et al. in *Gaussian 09 (Revision A.1)*, Vol. Wallingford, CT, 2009. For the complete authors' list, please see the Supporting Information. (c) Becke, A. D. *J. Chem. Phys.* **1993**, *98*, 5648. (d) Schaefer, A.; Huber, C.; Ahlrichs, R. *J. Chem. Phys.* **1994**, *100*, 5829.